Nationaal Lucht- en Ruimtevaartlaboratorium
National Aerospace Laboratory NLR

NLR TP 97147

The phase 2 up-grade of the NLR high speed tunnel HST

F. Jaarsma and A. Elsenaar

DOCUMENT CONTROL SHEET

	ORIGINATOR'S REF. NLR TP 97147 U		SECURITY CLASS. Unclassified

ORIGINATOR
National Aerospace Laboratory NLR, Amsterdam, The Netherlands

TITLE
THE PHASE 2 UP-GRADE OF THE NLR HIGH SPEED TUNNEL HST

PRESENTED AT
The European Forum on Wind Tunnels and Wind Tunnel Test Techniques organized by the Confederation of European Aerospace Societies (CEAS) on 14-16 April 1997, Cambridge, UK.

AUTHORS	DATE	pp	ref
F. Jaarsma A. Elsenaar	970312	20	9

DESCRIPTORS

Aerodynamic interference	Semispan models
Fan blades	Transonic wind tunnels
Flow stability	Wall pressure
Flow characteristics	Wind tunnel drives
Pressurizing	

ABSTRACT
The high speed tunnel HST of NLR has been in operation since 1959. Since its commissioning, the tunnel has played a major role in the development of many aircraft and missile configurations. In the eighties discussions started within NLR what modifications were required to meet industry requirements for wind tunnel testing up to the year 2000 and beyond. This has resulted in the phase-1 and phase-2 up-grade of the HST. The phase-1 up-grade, executed in 1992, was mainly focused on the test section, the model support systems and the tunnel control system. The site work for the phase 2 modification started in September 1996 and will last until April 1997. The main activity of the phase 2 up-grade concerned replacement of the power plant. For environmental reasons the present power house with 6 steam boilers could not be maintained. Hook-up to the public power grid was an attractive alternative which also provided the possibility to increase the maximum power from 15 Mw to 19 Mw. The new drive allows Mach control by rpm control so that at high subsonic speeds the fan efficiency will improve drastically. Since the fan blades and stator blades had to be replaced from fatigue considerations, it was decided to make a redesign with a further efficiency improvement. These changes resulted in a significant improvement of the working envelope of the HST in terms of Mach- and Reynoldsnumber. In particular the increase in Reynolds- number beyond Mach=.5 and the increase in maximum Machnumber to about 1.4 should be noted. As a consequence the cooling system had to be adapted. The test section and aerodynamic circuit are basically not changed except for installing a flow straightener with a set of new screens in the settling chamber to improve directional flow uniformity. Also the location of the halfmodel support is put more downstream to reduce buoyancy effects. Consequently, the high quality flow of the HST will be maintained or even improved. Finally, the new power system leads to a substantial reduction of cost of operations of the HST due to lower energy and personnel costs. Furthermore, it will also enable reduced starting and stopping times, resulting in a more efficient operation of the wind tunnel.

Contents

18 Figures

(20 pages in total)

THE PHASE 2 UP-GRADE OF THE NLR HIGH SPEED TUNNEL HST

F. Jaarsma and A. Elsenaar

Nationaal Lucht- en Ruimtevaartlaboratorium NLR
Amsterdam, The Netherlands

Abstract

The high speed tunnel HST of NLR has been in operation since 1959. Since its commissioning, the tunnel has played a major role in the development of many aircraft and missile configurations. In the eighties discussions started within NLR what modifications were required to meet industry requirements for wind tunnel testing up to the year 2000 and beyond. This has resulted in the phase-1 and phase 2 up-grade of the HST.

The phase-1 up-grade, executed in 1992, was mainly focused on the test section, the model support systems and the tunnel control system.

The site work for the phase 2 modification started in September 1996 and will last until April 1997. The main activity of the phase 2 up-grade concerned replacement of the power plant. For environmental reasons the present power house with 6 steam boilers could not be maintained. Hook-up to the public power grid was an attractive alternative which also provided the possibility to increase the maximum power from 15 Mw to 19 Mw. The new drive allows Mach control by rpm control so that at high subsonic speeds the fan efficiency will improve drastically. Since the fan blades and stator blades had to be replaced from fatigue considerations, it was decided to make a redesign with a further efficiency improvement.

These changes resulted in a significant improvement of the working envelope of the HST in terms of Mach- and Reynoldsnumber. In particular the increase in Reynolds- number beyond Mach=.5 and the increase in maximum Machnumber to about 1.4 should be noted. As a consequence the cooling system had to be adapted.

The test section and aerodynamic circuit are basically not changed except for installing a flow straightener with a set of new screens in the settling chamber to improve directional flow uniformity. Also the location of the halfmodel support is put more downstream to reduce buoyancy effects. Consequently, the high quality flow of the HST will be maintained or even improved. Finally, the new power system leads to a substantial reduction of cost of operations of the HST due to lower energy and personnel costs. Furthermore, it will also enable reduced starting and stopping times, resulting in a more efficient operation of the wind tunnel.

Symbols

C_D	Drag coefficient
C_l	Lift coefficient
C_p	Pressure coefficient, $\Delta P/q$
h	Test section height
k	Pressure drop across screen, $\Delta P/q$-local
l	Characteristic length
Ma	Machnumber in the test section
n	Rotational speed of fan
p	Pressure
P_0	Total pressure
P_{0u}	Total pressure upstream fan
P_{0a}	Total pressure downstream fan
q	Dynamic pressure
R	Gasconstant
Re	Reynoldsnumber
T_0	Total temperature
$U_{\text{wall interference}}$:	Induced axial speed at test section axis due to wall effects
U_s	Axial flow speed
V_t	Fan tip speed
x,y,z	axial, lateral, vertical co-ordinates
$\Delta\alpha$	Flow angle deviation in pitch direction
$\Delta\beta$	Flow angle deviation in yaw direction
η	Fan efficiency
ψ	Dimensionless fan pressure rise $\{(P_{0a}/P_{0u})^{2/7}-1\}RT_0 7/V_t^2$
φ	Fan advance ratio U_s/V_t

Abbreviations

ABB	Asea Brown Boveri
ARA	Aircraft Research Association
DNW	German Netherlands Windtunnel
ETW	European Transonic Windtunnel
HP	Horse Power
ILST	Indonesian Low Speed Tunnel
LST	Low Speed Tunnel

NOX	Nitrogen Oxides
PHST	Pilot High Speed Tunnel
rpm	Rotations per minute
TLT	Turbo Lufttechnik
SST	Supersonic Tunnel

1. Introduction

The high speed tunnel HST of NLR has been in operation since the early sixties and has made many contributions to European aerospace projects. In the eighties it has been decided to up-grade the facility to better meet the requirements as put forward by the industry in terms of improved accuracies, capabilities and economics. Because of budget constraints a first phase of modernization was executed in the early nineties and this mainly included adaptation to the test section, model supports and control systems.
In ref. 1 this phase has been reported and in ref. 2 the results of this up-grade has been presented. In this last presentation also a forecast was given of a possible improvement by the second phase up-grade. Fig. 1 presents the airline diagram. The test section is 2 m wide and two heights can be used: 1.6 m (original) and 1.8 m as introduced during the first phase up-grade.

This second phase up-grade came earlier than initially foreseen. Soon after the first up-grade was completed the Dutch authorities announced that the smoke emission of power plants had to meet very narrow limits by the year 1998. Since the HST was powered by a self operated steam boiler power plant this would have strong consequences for NLR. In particular the NOX emissions were of concern. The existing limit was 700 mg NOX/m^3 [i]. The average actual emission of the power plant was about 300 mg/m^3 and this had to be reduced to 200 mg/m^3. Consultation with boiler and burner suppliers revealed that a 30 percent reduction of NOX emission could be achieved by exhaust gas recirculation (reducing flame temperature). No guarantee could be obtained to really achieve this limit mainly because of the volume limitations of the existing boiler furnaces.

Contacts with the municipal power supplier in the past learned that it would be very expensive to have a connection to the local power grid because a special long high voltage power cable had to be drawn from the most nearby power plant. Renewed contacts with the local power supplier learned that the situation had drastically changed in recent years and a nearby substation had sufficient power to serve NLR.

So the decision was soon made to hook-up to the local power grid and to shut down the power plant. Besides negotiations with the power supplier resulted into attractive power tariffs as compared to the costs of power generated up till now by ourselves, in particular when power is extracted when the public power consumption is low such as during the evenings, nights and week-ends.

In fact, a wind tunnel is not a major energy consumer because of the relatively short full power operation periods. A wind tunnel is a power consumer with short start-up and shut-down times. Nowadays a dedicated steam boiler power plant turns out to be not compatible with the power demands of a wind tunnel because a steam boiler requests long start-up and shut-down times which results into long stand-by times. Moreover the overall energy efficiency was relatively low. Better suited to drive a wind tunnel is a gasturbine or a diesel engine power plant, but in both cases this would require large investments and on top of that emission constraints will remain. Since power generation is not NLR's core business, hook-up to the public power grid was the best solution.

The HST was originally designed for 25.000 HP or 19 MW but initially only 20.000 HP was installed, divided over 4 engines of 5000 HP in a tandem arrangement (fig. 2). Switching to the public power grid also required new electric drive motor(s) because of frequency differences and degraded quality of the insulation of the engine wiring. Thus the opportunity arose to install a drive giving 19 MW to the fan shaft with variable frequency. To this end the fan should also be adapted as explained in the next chapter.

It was estimated that the switch to a new power source and new drive would require a shutdown of approximately 6 months. Thus, the opportunity arose to up-grade other items as well such as the flow quality, halfmodel testing capabilities, flow visualization capabilities and productivity. These aspects are treated in the subsequent chapters.

2 Improvements to the fan

2.1 Historical review

The HST fan was initially designed to have maximum efficiency (82%) at maximum supersonic Machnumber (1.37) in the test section. This required a fan (total) pressure ratio of 1.35 and still giving a stall margin of 35%. The HST fan had 4 stages, each containing 22 blades and the fan speed was fixed at 620 rpm, which

is relatively moderate for a 4.8 m diameter fan; hub to tip ratio 0.66. Mach and speed control was achieved by blade pitch control over a range of approximately 60 degrees. Simultaneous blade pitch movement is provided by a single low pressure hydraulic drive in the fan rotor. The fan could run at lower rpm with the consequence of a proportionally lower available power.

The fan electric drives on the single shaft were synchronous motors and the speed was dictated by the frequency of an average of the four steam turbine driven generators. So, rpm control of the fan was actually done by the steam turbine throttling valves. Hence it can be imagined that the rpm could not be held as constant as was desirable. Besides the power line was weak, meaning frequency decrease at extra power demand. Although rpm variation could be compensated fast enough by blade pitch adjustment, this demanded a high performance control system.

Another important aspect for the fan and drive is that the HST is a pressurized wind tunnel. The total pressure can be selected between 0.2 and 3.9 bar absolute. The required power at a certain Machnumber is proportional to the total pressure. For transport type aircraft the region of interest for wind tunnel testing is around M=0.8. This value requires a fan pressure ratio to drive the tunnel between 1.08 and 1.10 (depending also on model attitude). At these pressure ratios the fan efficiency turned out to be very low as may be seen in fig. 3a. Fans usually show maximum fan efficiency between 70 and 80% of the stall value. Reduced fan speed and/or reduced number of blades increase efficiency at high subsonic speeds and with that the effective aerodynamic power. The maximum effective aerodynamic power determines the maximum total pressure (and hence max-Re) that can be used. This is demonstrated in the Mach-Re diagram of fig.4.

The above argument led in the eighties to the decision to halve the number of blades of the HST fan by deleting the second stage entirely and to halve the number of blades of the third and fourth stage. This improved substantially the subsonic performances, about 20% in Reynoldsnumber as is depicted in fig. 4, but degraded the supersonic capabilities since the maximum fan pressure ratio was reduced to 1.19.

2.2 New fan design

Although the efficiency of the fan was improved by blade number reduction as discussed above, at high subsonic speeds the fan was still marginal with regard to what could be expected from a modern fan (fig. 3b). Therefore, with the decision to switch over to the public power grid it was logical to optimize the entire drive-fan train. To this end the German company Turbo Lufttechnik GmbH, TLT, (successor of the original supplier Dinglerwerk A.G.), was requested to execute a feasibility study with the following objectives:

- at a fan pressure ratio of 1.1 the fan efficiency should be at least 80 percent, preferably 85 percent (at an airspeed through the fan of 70 m/s)
- the maximum fan pressure ratio should be at least 1.27, preferably in excess of 1.3 (at airspeed through the fan of 80 m/s).
- the stresses in the guide vanes should be reduced to such levels that fatigue cracks will not occur anymore

The condition was to keep the fan housing and rotor in existence as much as possible including the blade pitch mechanism.

From this study it was concluded that:

- the objectives could not meet with a single speed drive
- the existing blades could not be reused because of performance and strengths limitations
- a dual speed motor with pole rearranging at stand-still was not a viable solution at these large powers.
- a variable speed drive was the only solution to meet the objectives
- the maximum allowable shaft torque was the limiting factor for the minimum speed at maximum power.

In close consultation with TLT, considering five alternative solutions for the fan-drive combinations, it was decided to:

1 provide three stages with full blading (22) of a new design (all equal blades)
2 renew the stator vanes
3 operate the drive at maximum power (19 MW) between 470 and 650 rpm
4 renew the drive shaft to accommodate the required 65% higher torque levels.

The new aerodynamic design of the fan was based on earlier designs by TLT (designated DA). Fortunately TLT was still in possession of a model of the HST fan and by inserting new model blades in the three stages the aerodynamic performance was confirmed in a model test (fig. 5). Translating these results into the HST Mach-Re performance diagram resulted in the envelope as shown in fig. 4. No account has been given for the differences in Reynoldsnumber, blade tip

[i] A standardized m^3 based on oxygen content

and root clearances and flow obstructions in the actual fan. It is expected that these effects will balance. The final performance tests will give the real answer. The electrical, shaft and aerodynamic power will be measured during commissioning.

2.3 The blades

The old blades were made of steel sheets welded to internal frames and a spar. The spar extended into a spoke that was supported at the blade root by a radial and at the free end by a radial and axial bearing. At the free end a lever was connected for blade pitch control. The steel blades were sensitive to material fatigue. During the annual overhaul sometimes cracks in the steel plating had to be repaired.
For the new blades the following material options were considered:
- solid aluminium
- solid titanium
- fibre epoxy composite.

The last option was selected, also because NLR has ample and good experience with (carbon) fibre blades for model propellers and model helicopter rotors (for the DNW) as designed and built in house (without any accident with these blades). It was agreed with TLT that NLR would design and manufacture the new blades under supervision of TLT. This was done and the prototype blade withstood statically 6 times the maximum load and dynamically 2 x 10^6 cycles of maximum load plus + and - 150 percent (so load variation from - 0.5 till + 2.5 times maximum load).

The blade itself has a machined core of Rohacell 71 in which tapered carbon fibre bars under the skin forms the spar (fig. 6). The skin is made of aramide fibres, 2 mm thick and strengthened at the trailing and leading edges. The outer surface of the skin is made of glass fibre cloth to assure a smooth surface. The curing of the fibre and the core material is done in one piece in a mould consisting of two negatives of carbon fibres pressed together in an oven. Two blades per day could be produced. The overall costs turned out to be less than half of the nearest price proposal.
The fact that the dynamic loading may also be negative gives a special constraint for the fibre composite-spoke connection near the blade root. For this reason a pin connection was selected: three steel pins in a row (see fig. 7).

During commissioning the aerodynamic loads on the blades will be monitored by strain gauges to verify whether the dynamic loading during the fatigue tests has been sufficient. In particular the dynamic loading near stall is of importance. Stall testing will be done initially at low tunnel pressures.

2.4 Stator vanes

The fatigue crack situation was even worse for the stator vanes (47 vanes per stage). These vanes consisted of single 8 mm steel plating, bend over a circular arc (with a twist) and were directly welded to the outer and inner casing; the latter containing a labyrinth to seal the airpassage to the former stage. The vanes showed severe crack development in all four corners and required replacement anyway because the material was completely dead due to the many welding repairs.

Vibration measurements on the stator vanes prior to shutdown learned that occasionally the stator vanes came into severe resonance in the first torsional mode. The resonance frequency was lower than the blade pass frequency. The amplitudes were that large that by this phenomenon the large stresses in all four corners could be explained. The problem is cured by connecting the new vanes to each other by stiffening plates in a staggered way (see fig. 8) such that the natural frequency of the first torsional mode will be tripled, well in excess of the blade pass frequency.
The Dutch authorities (Stoomwezen) allowed to reuse the outer casing of the fan house (without pressure testing) if the new vanes were welded at new positions to the casing in between the positions of the former vanes.

In order to properly execute this work, the entire fan housing had to be dismantled so that the repair and welding operation could be executed in a work shop under controlled conditions to minimize distortions due to welding. This operation has been successful and the blade root and tip clearances could be set to minimal 2 and 3 mm respectively (average 3.9 mm), being essential for good fan efficiency.

3 Improvements in flow quality

3.1 General

Flow quality in the test section can be expressed in the following identities:
A Reynoldsnumber
B Machnumber and Machnumber stability
C Total pressure distribution
D Static pressure distribution (and stability)
(C and D together gives the Machnumber distribution)

E Temperature distribution and stability
F Flow angularity
G Turbulence
H Noise and spectra

The identities C, E, F, and G are determined by the level of flow conditioning in the settling chamber and by the contraction ratio. The contraction ratios are respectively 25 to 1 and 22.2 to 1. The identities A and B are determined by the test section size, pressure, fan characteristics and available power as discussed in the previous chapter except for Machnumber stability. The identities D and H are dependent on the test section geometry and the flow re-entry. The ceiling and floor are slotted (12.5% open) and the side walls are solid. The settling chamber contains a two row heat exchanger followed by five fine anti-turbulence screens with a k-value of about 1. Upstream of the heat exchanger a course screen is placed in the wide angle diffusor to spread the flow properly over the heat exchanger face without separations.
The large contraction together with the inserts in the flow in and upstream of the settling chamber assured low turbulence levels (G) and a uniform total pressure (C) in the test section as has been observed.

The various identities will be discussed next.

3.2 Reynoldsnumber

This has been discussed already in the previous chapter. It is repeated here that it is expected that the maximum Reynoldsnumber at high subsonic speeds will increase about 50%: 25% due to power increase and 25% due to improved fan efficiency by running at lower fan speed and improved fan and vane geometry. For full models a Reynoldsnumber of 6 mio (c=0.17m) will be attainable, for halfmodels 12.5 mio (c=0.35m), both in the Machnumber range from 0.5 till 0.85. This last value is already about 50% of the full scale value for say a 100-seater passenger transport and usually well beyond a critical value for reliable prediction for fullscale by computation and/or extrapolation from lower Reynoldsnumber data by pressure level variation (ref. 2).

3.3 Machnumber

The maximum attainable Machnumber depends on the maximum pressure ratio the fan can generate. This value will increase from 1.19 to about 1.3 and this will allow operation up to Machnumber of 1.37 with a test section height of 1.8 m. The maximum Machnumber will also depend on the model support boom and model to be in use and the position thereof (ref. 1). The actual values will be determined during commissioning.

Another aspect is Machnumber stability. This is divided into:
- stability during a model polar sweep
- stability at model in rest.

It is generally required to keep the Machnumber within ± 0.001 of the setpoint. The first stability problem is associated with drag variation during a sweep (e.g. in incidence). The fan pitching mechanism is sufficiently fast to cope with this problem but this results into power variation and as a consequence in a rpm variation. Besides, the power change rate of the former steam boiler power plant was limited (thermal inertia effects) and this in fact limited the maximum allowed sweep rate of the model. Nevertheless, the Machnumber/ blade pitch control system was essentially capable to keep the Mach constant within the margin as given (0.001). With the new drive the rpm will be held constant within 0.5 rpm by digital means and this will highly lighten the performance requirements of the Machnumber control system.

The second stability phenomenon is more random with a frequency level of a few Hz and less. It is associated with the flow re-entry and the phenomenon is observed as a fluctuation of the plenum pressure which is essentially the static pressure of the flow in the test section. For certain circumstances the Machnumber can fluctuate as a result of this plenum pressure fluctuation as much as 0.003 in Machnumber.

ETW has prevented this phenomenon by using a second throat just downstream of the re-entry (ref. 3). The HST has no second throat and besides, a second throat consumes much power because of shock losses. The ARA has coped with this problem by a fast control of an air bleed system from the downstream location of the fan to the plenum (ref. 4) This active control was able to keep the plenum pressure well within the given margins, but this bleed affected the buoyancy in the test section (axial static pressure gradient). Therefore the drag data had to be corrected for the actual position of the control valve in the air bleed.

NLR will follow the solution as used by ARA. It has been demonstrated in the HST that the plenum pressure level can be affected sufficiently fast by suddenly opening of a 50 cm^2 valve between the settling chamber and the plenum. The system will be designed to suppress Machnumber variations up to

0.005 by operation of a 100 cm^2 fast valve which is on average half opened. This will cause some loss in available power but this will be less than 1 percent of the drive power. The valve will actually be a digital valve consisting of 20 one-inch fast acting (25ms) open/close valves in parallel. Opening of the 50 cm^2 valve did not have an effect on the buoyancy. The mass flow through the air bleed is only 0.15% of the main flow and this amount will hardly effect the re-entry flow. The main problem will be to tune this fast Machnumber control with the slower Machnumber control by blade pitch adjustment which also incorporates a delay due to the large distance from the test section.

3.4 Static pressure distribution/ wall effects for halfmodels

The test section is not modified in this upgrading campaign except for the wall (port side) containing the halfmodel support. The reason is explained next.

In the phase 1 up-grade the support strut was moved downstream and the test section length was increased with 1.15 m (ref. 1). The reasoning for the increased test section length was to move the nose of the model away from the transition between the closed nozzle and slotted part of the test section. It was well known that this transition introduced unwanted buoyancy forces caused by a pressure gradient that depended on the model position, the blockage ratio and the Machnumber. The validation experiments confirmed that this unwanted effect could be eliminated: the drag polars were identical when the model position was varied except for the most forward model position (ref. 2).

Although this improved the situation drastically for full models, the model position for half models and two-dimensional models remained unchanged. The HST has large turntables in its side walls for mounting two-dimensional models across the test section or halfmodels against the port wall. For Reynoldsnumber studies, use is made of large halfmodels and two-dimensional models. The halfmodels are sometimes so large that the nose "touches" the solid nozzle and from various studies (e.g. ref. 5) it was known that this introduced large buoyancy effects on the halfmodels. In fact, a special technique was developed to correct for these effects. Hence, a more downstream displacement of the halfmodel would have been very beneficial. However, in the phase 1 up-grade, the location of the turntables remained unaffected and it was later decided to redress this situation during the phase 2 up-grade.

The occurrence of pressure gradients at the solid nozzle/slotted wall transition is well illustrated by some experiments made in the Pilot HST (PHST). This tunnel, an 1:4.16 scaled version of the HST, was used to guide the aerodynamic up-grade of the HST test section. Some of these studies were done with a high lift model, specifically designed to assess wall interference. The model could be positioned in a forward and central position and this has a very large effect on the upstream pressure distribution measured at the top and bottom walls (fig. 9). In this figure, the wall pressure distributions have been plotted relative to the model itself for different open area ratio's of the slots. Note that the pressure coefficient C_p is defined relative to the plenum pressure. The figure hence indicates a higher pressure in the closed nozzle relative to the plenum pressure. Moving the model forward increases this level drastically. Making the slots more open reduces this effect. It is of interest to note here that the pressure distribution on the walls near the model remained almost unchanged. The high upstream value of C_p introduces a pressure gradient over the nose of the model, resulting in strong buoyancy effects.

It should also be noted that a careful comparison between model tests in the PHST and the much larger HST had revealed that an open percentage of 12.5 % virtually eliminated all lift interference effects. Therefore a further increase in slot width was not considered.

Consequently, a more downstream displacement of the halfmodel was the best option to reduce the pressure gradient effect. Wall interference studies on halfmodels in the HST before and after the phase 1 up-grade have supported the PHST experiments. Figure 10 shows the pressure distribution for a large halfmodel (1.7% blockage, wing area 10% of the cross sectional area) as measured in the HST. With this halfmodel a similar variation in wall pressure distribution was observed as the one shown in figure 9. Note that the upstream effect is largely due to the presence of the fuselage whereas the effect of the wing is mainly felt close to the wing location.

From the measured wall pressure distributions and an accurate representation of the model, the wall interference effect along the model axis has been calculated (ref. 6) and this is illustrated in figure 11. The figure shows the model induced velocity component in free stream direction ($U_{\text{wall interference}}$).

This has been calculated after the phase 1 up-grade from the respective halfmodel tests. Also, the situation with an increased test section height (from 1.6 to 1.8 m) has been indicated. The figure illustrates the large gradient along the model axis especially in the nose region.

Based on these studies it was decided to move the halfmodel mounting position .55 m downstream but to keep the original forward position also possible. The turntable in the forward position has to remain operable to mount 2-D models. It turned out to be very cumbersome and hence expensive to remount the turntable in the access door on the starboard side of the test section. Fig. 12 shows how the port wall has been modified for the two possible positions of the turntable.

It is clear from the above discussion that it cannot be expected that the wall interference effects will be completely eliminated. But it is also clear that a significant reduction of the upstream pressure gradient effect can be expected, an effect that can be further reduced by using the option of increased test section height. It is hoped that the remaining wall interference effects are such that wall interference correction methods based on measured wall pressures can accurately correct for the remaining buoyancy effect.

3.5 Temperature distribution and stability

3.5.1 Air temperature level The HST is cooled by fresh channel water from a nearby harbour, directly pumped through the heat exchanger at a flowrate of 0.5 m^3/s. By increasing the power one would expect a temperature rise of the tunnel air flow. The necessary heat transfer (being at steady state equal to the power input) between the channel water temperature and the tunnel air total temperature is governed by the difference between the average water temperature and average air temperature across the heat exchanger. However, the overall heat transfer coefficient of the heat exchanger will also increase with power input because of the proportionally increase in air density (the heat transfer coefficient at the air side is the dominant factor). The boundary layer on the fins of the heat exchanger is partially laminar and partially turbulent and it is experienced that the heat transfer coefficient is proportional to the air density to the 0.65 power (0.5 for laminar, 0.8 for turbulent boundary layer). So, for an increase in the air density by 25%, resulting in 25% power increase at a certain Machnumber, the heat transfer coefficient increases with 16%, which results in an increase of the average temperature difference across the heat exchanger of only a few (2) C. The average water temperature will increase with 1 C so that the tunnel air temperature would rise only about 3 C.

However, the water entry temperature will decrease about 1 C because the former arrangement with the steam boiler power plant was such that part (15%) of the water outlet was re-ingested as water inlet flow (see fig. 13). Besides, the heat exchanger has been thoroughly cleaned, both internally and externally which has a beneficial effect on the heat transfer coefficient. There were strong indications that some finned water tubes were clogged. So, it is expected that the total air temperature will hardly be higher after the up-grade using the higher power level. Besides, it was experienced before that during the course of a testing day the air temperature rose slowly a few degrees because water re-circulation in the harbour. This will hardly happen again because the heat input to the water will be reduced an order of magnitude with the shutdown of the steam boiler power plant.

3.5.2 Temperature stability Temperature control could be achieved in the past by water bypassing the heat exchanger. This in turn had a negative effect on the air temperature distribution. Besides, the bypass control valve could not respond fast enough to the power variation, and hence air temperature variation, during a polar sweep. Therefore, it gradually became practice in the past to apply full cooling all the way through the test program. This was acceptable because the newer model balances and other instrumentation became less sensitive for temperature gradients.

Air temperature control is most optimally achieved by cooling water temperature control. For practical (constructional) reasons it was cheaper to leave the main waterpump(s) at place and extend the outlet piping. This gives a much too long (~ 1 min.) response time. Therefore, it was decided to install as close as possible to the heat exchanger a re-circulation pump with a three way control valve (fig. 14). The control simulator of the cooling system recorded an essential improvement (fig. 14). The objective is to achieve temperature stability within 1 C during a wind tunnel run.

3.5.3 Temperature uniformity Tests, just prior to shut-down revealed that the air uniformity has degraded in the past. Total air temperature differences in the flow as large as 3 C were recorded. During commissioning the waterflow rates through the various bundles will

be tuned at an average tunnel usage condition (around M=0.8) with the objective to achieve temperature uniformity within ± 1 C. In particular the water flow rate in the exchanger bundles near the side walls requires water flow reduction. Besides, the effect of the cleaning operation can be observed during the commissioning.

3.6 Flow angularity and turbulence

Flow angularity and turbulence are different phenomena in the flow, but both are affected strongly by the same measures to be taken in the settling chamber. Five hole probe traversing tests in the test section, prior to shut-down have revealed that at some locations the flow angle deviation from average were more than the generally accepted value of 0.1 degree. Inspection of the fins of the heat exchanger and quality of the screens made it obvious that such deviations could be expected as found from past experience with the development of new low speed tunnels (DNW, LST, ILST) (ref. 7).

The flow speed in the settling chamber of these low speed tunnels are very similar to that for the HST and therefore, it was decided to adapt for the HST the flow conditioning solution as used in these low speed tunnels, which are known for their low turbulence levels and good flow angularity.
So, the following was done:
- removal of all five settling chamber screens
- installation of a flow rectifier in the form of honey comb panels (d cell ½", L/d=10) directly coupled to the heat exchanger structure
- re-installation of three anti-turbulence screens having a k-value of 1.0 and a mesh size that has been used for the LST (mesh 1.27 mm, wire diameter 0.4 mm).

As reported in ref. 7 a flow rectifier also strongly suppresses lateral turbulence, whereas screens provide flow uniformity across its surface and suppress axial turbulence. One could argue that screens could be obsolete for turbulence suppression (because a contraction suppresses axial turbulence more than lateral turbulence) but the flow rectifier support structure will cause wakes and additional turbulence that have to be damped by screens. Therefore three new screens are installed downstream of the flow straightener.

On the other hand, screens, even carefully made, have a tendency to deteriorate flow angularity. There is evidence that the weaving direction has an effect on flow angularity. As reported in ref. 7 local flow angle deviation in weaving direction tends to be larger than the deviation in woof and weft direction of the screen. This expectation has been confirmed in a recent test in the LST (fig. 15) and therefore the new screens in the HST are assembled of three horizontal screen sheets with two seams, one above and one below the center. The seams are plasma welded, wire by wire, and are hardly visible. Nevertheless the vertical positions of the seams are staggered for the three successive screens.

4 Improvements to increase productivity

With the installation of the new drive hooked-up to the public power grid the start-up and stopping times will be dramatically shortened from typically 15 minutes to 2 to 3 minutes. Also the adaptation to the cooling system as mentioned in section 3.5.2 and the improvements in the Machnumber control system will allow faster movement inbetween setpoints for successive polars. Also the sweep rate during a polar can probably be increased. Experience will show how far this will be possible.

Pressurization of the tunnel is achieved by charging from the 600 m^3, 40 bar pressure vessel that is also used for running the blow down supersonic tunnel SST. Charging from atmospheric pressure to 3.9 bar took 17 minutes. By re-arranging and implementation of a dedicated pressure controller the charge time will be reduced to 8 minutes.

It has been considered to install large gate valves in the nozzle and in the re-entry area to save pressurized air in the shell, but this would be not cost effective, and besides would not help when pressure changes are required for the various polars during a run.

Of course, with the new drive system, the MMI (Man Machine Interface) has to be adapted and where possible the tunnel will be operated in the fully automated mode (ref. 1).

5 Other related changes

5.1 Drives

The new drive is one single motor which supplies the maximum power between 470 and 650 rpm. The supplier is ABB and the motor is of the synchronous type with a Load Commutated Inverter (LCI).

The drive is located in a new housing in between the

former motor house (with the four engines) and the HST shaft penetration at the second corner. Hence the new drive shaft is shorter. Underneath the new drive at ground level, the new 50/11 kV, 30 MW transformer is located and the former motor house is reconstructed to contain the middle tension switch gears, frequency converter and dedicated transformers of the drive. The fan and drive shaft are protected from short circuit torque by a safeset coupling.

The shutdown of the steam boiler power plant also required new drives for the two large 40 bar air compressors (resp. 7 and 8 kg/s) to charge the 600 m^3 air vessel. These compressors were driven directly by steamturbines of 5 MW. In the new situation the air compressors each are driven by two 2.5 MW DOL (direct on line) engines fed by 11 kV. The low pressure stages of each compressor is driven by an electric motor via a dedicated gearbox as well as the middle plus high pressure stages (see fig. 16).

5.2 Instrumentation

Because of the higher q values that can be generated, the flow reference system also had to be up-graded. Double ranging is necessary now to achieve sufficient accuracy over the entire range of total pressures and static pressures. Tubing is established such that equal or at least comparable response times can be attained.

Besides the total pressure and temperature probes are relocated to better establish the mean flow reference values and to interfere least with the flow prior to entering the contraction.

The work in the settling chamber gave the opportunity to install a fixed smoke injector upstream of the heat exchanger. The location and way of smoke injection has been established in trial tests in the available pilot facility (PHST) developing the PIV techniques and these findings were later confirmed in the HST in a commercial test using an improvised injector (fig. 17). The permanent ejector can provide seeding at any location in the test section over a distributed area as desired.

The higher dynamic pressures will give also higher loads on the models and therefore new full model and halfmodel balances are designed and are under manufacture. The new high load balance for transport type models is almost ready for calibration. The available stings can absorb the higher loads for the time being. The model support mechanism and the booms were already designed for the higher loads during the first phase of modernization (ref. 1).

Upon becoming ready for commercial testing the model attitude measurements by inclinometers (Q-flex) will be improved by compensating for errors which arise from model vibrations (ref. 8, 9). Besides the number of measuring channels will be increased to sixty and the data flow organization to the data acquisition system will be improved to handle more and data of different signature.

5.3 Fan protection

Formally the HST had two safety screens to protect the fan; one coarse screen (10 cm holes) at the downstream end of the first (test section) diffuser and a fine screen (1 cm mesh) connected to the vanes in the second corner. Both screens (in particular the first one) had to be frequently repaired because of fatigue ruptures especially when heavily loaded model tests were executed.

It is expected that the situation will become worse with the 50% higher possible aerodynamic loading. Therefore it was decided to install instead one single protection device in between the second corner and the fan, similar as executed at ETW. The protection device consists of 3/8" cell alu honey comb panels (depth 200 mm) contained in a web-type structure. Before implementation hereof free-fall impact tests have been carried out to demonstrate the detaining capability (fig. 18). The heaviest impact was a simulated 3 kg sphere at a speed of 30 m/s. As a result of these tests the bonding between the honey comb and the frames has been improved.

5.4 Corner vanes

The corner vanes of the HST consists of steel (6 mm) plates bend over 90 degrees, similarly as reported in ref. 7. The vanes are interconnected at some locations by splitter plates and stiffened in between by horizontal plates. Occasionally these vanes in the first and second corner showed fatigue crack development both at the leading and trailing edges. Because of the 50% higher aerodynamic loads after up-grade the situation would become worse.

Vibration measurements during regular model testing has revealed that both the trailing and leading edges were irregularly vibrating by aerodynamic excitation, but there was no coherence with pressure fluctuations. The middle curved parts of the vanes were relatively

quiet, so the torsional modes were not excited. It was therefore decided to add extra stiffening plates (about double) and according to computation the problem should be solved.

5.5 Wide angle diffusor screen

The seams in the wide angle diffuser screen were originally of the sewed type. The screen was made of 0.7 mm phospherbronze wire. Since these seams were repaired in the past, there was an uncomfortable feeling applying these seams to the higher aerodynamic loads. Therefore it was decided to repair these seams by in situ plasma welding of new seam strips. When executing this work it appeared that at some edges near the walls the wires were broken because of fatigue and wear due to apparent vibrations. It was then decided to renew the entire screen with welded seams. The static strength is by far sufficient as could be concluded from pressure drop measurements across the screen.

5.6 Final remark

The topics mentioned in the preceding sections of this chapter cover the changes that have been made because of the experience gained in the past and the higher aerodynamic loading beyond the up-grade.

All relevant components in the circuit have been critically reviewed to establish whether the higher loading will or will not effect the safety of operation. Except for the above mentioned topics no critical parts are noted. Nevertheless, during the commissioning any uncertain part will be monitored, mainly by vibration analysis.

6 Concluding remarks

With the completion of the 2nd phase up-grade of the HST this tunnel can be considered as one of the most modern high speed tunnels in the world with very attractive performance characteristics, high productivity, good economics and producing high level data. Of course, the final characteristics still have to be established during the commissioning (that will have just been started at the presentation of this paper at the conference) and calibration campaign. Also some fine tuning, for example of the control systems, may take some time beyond commissioning but the prospects for a good result are promising.

The above statements lead also to the conclusion that the basic layout of the 40 year old HST was good and is still modern. A modern facility could be attained in the two up-grade campaigns for a fraction of the costs for an all new facility.

As with any re-construction project unexpected problems showed up, more than in "all new" construction projects. Problems were encountered due to lack of "As built" drawings (not done in the fifties), inclusions in material for major components, loss of reference data due to disassembly and last, but not least, due to severe strong freezing weather conditions. Nevertheless the project remained quite well within budget and schedule.

Acknowledgement

The authors wish to thank all those who were involved in the HST up-grading, phase 2. In particular the detailed site co-ordination of the deputy project manager, Ing. J. van der Spek, is much appreciated. The company TLT should be mentioned for making available the fan data.

References

1 F. Jaarsma, J. Smith, R.K. van der Draai: "A modernized HST of NLR", European Windtunnels and Forum on Windtunnel Test Techniques. Southampton University U.K. 14-17 September 1992.

2 A. Elsenaar, F. Jaarsma, "The Modernization Program of the Transonic Windtunnel HST of NLR: Lessons from the Past, Prospects for the Future", 19th ICAS Congress, Anaheim, USA, 18-23 September 1994.

3 X. Bouis, J.A. Tizard, G. Hefer, "ETW Aerodynamic Design - A case Study -" AGARD FDP meeting, Aerodynamics of Wind Tunnel Circuits and their Components, Moscow, 30 September - 3 October 1996.

4 E.C. Carter, K.C. Pallister, "Development of Testing Techniques in a Large Transonic Wind Tunnel to Achieve a Required Drag Accuracy andFlow Standards for Modern Civil Transports", AGARD FDP meeting, Napels, 28 September - 3 October 1987. CP 429.

5 S.J. Boersen, A. Elsenaar, "Half-Model Testing in the NLR High Speed Windtunnel HST: Its Technique and Application", AGARD CP 348 (1983).

6 R.A. Maarsingh, "Wandinvloedsberekeningen met WIN3VE ten behoeve van metingen aan halfmodellen F28-17-9 en F28-17-10 in de HST", NLR Internal Memorandum AX-95-002 (1995) (in Dutch).

7 F. Jaarsma, "General Design Aspects of Low Speed Wind Tunnels", AGARD FDP meeting Aerodynamics of Windtunnel Circuits and their Components, Moscow 30 September - 3 October 1996.

8 P.H. Fuykschot, "Vibration Compensation of Gravity Sensing Inclinometers in Windtunnel Models", NLR TP9600 3L (Presented at 42nd International Instrumentation Symposium, San Diego, 5-9 May, 1996).

9 P.H. Fuykschot "Looking for the Last Drag Count-Model Vibrations vs Drag Accuracy", NLR TP9648 5L (Presented at International Symposium on Strain-Gage Balances, NASA Langley, 22 - 25 October, 1996).

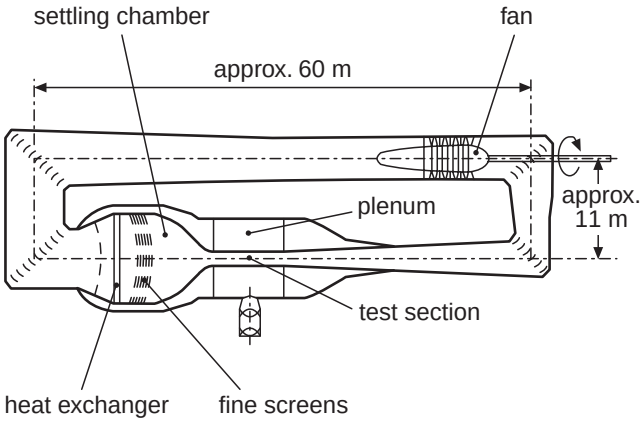

Fig. 1 High Speed Tunnel HST

Fig. 2 Former main drive system

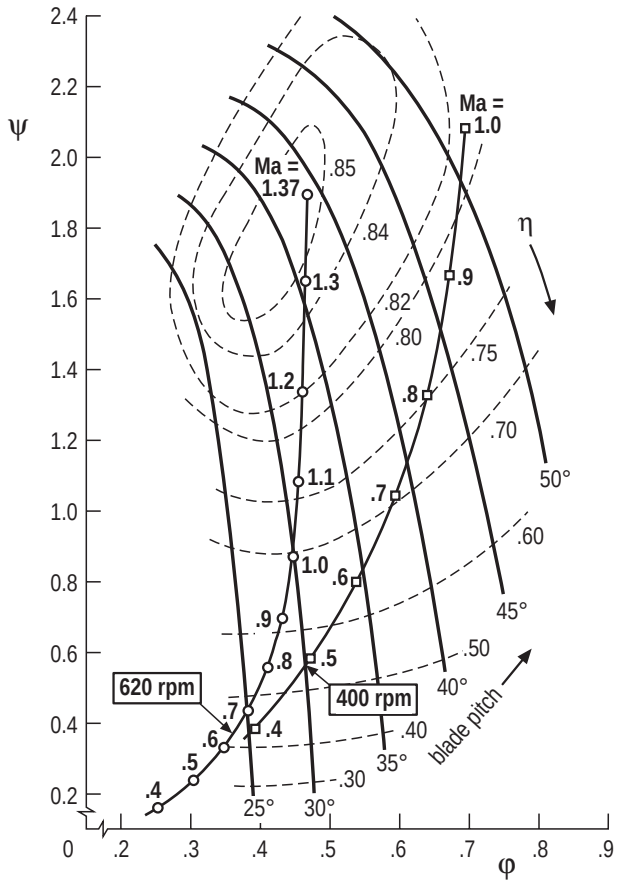

Fig. 3a Characteristic of original fan, 4 stages, 22 blades per stage

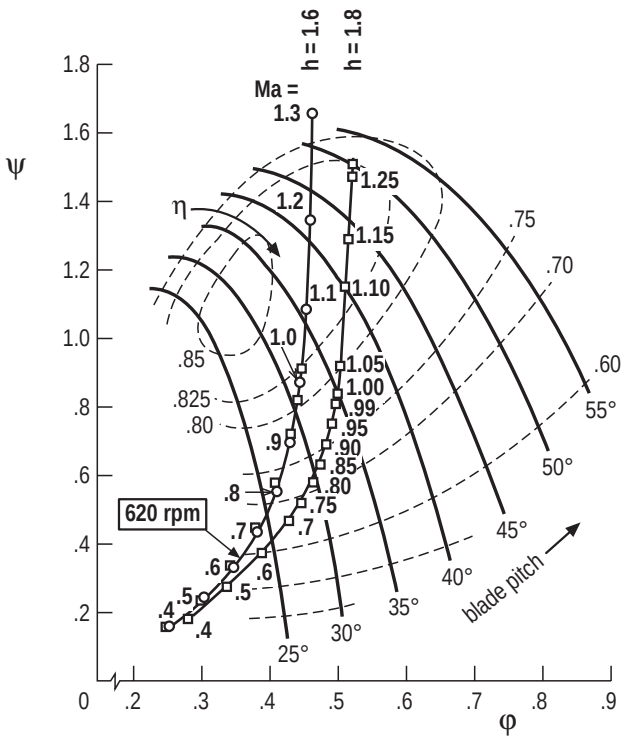

Fig. 3b Fan characteristics after blade reduction

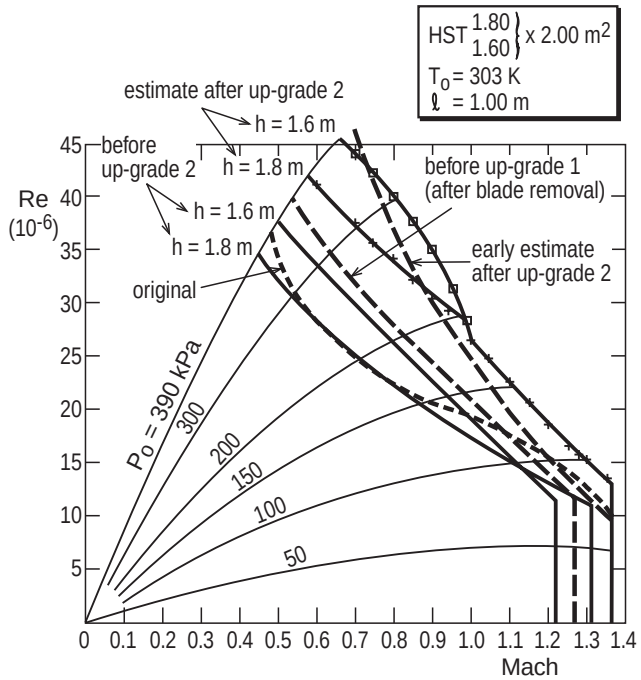

Fig. 4 The Reynolds number as a function of the Mach number in empty test section, originally, after blade removal (before up-grade 1), before up-grade 2, estimated after up-grade 2 (estimate from model tests)

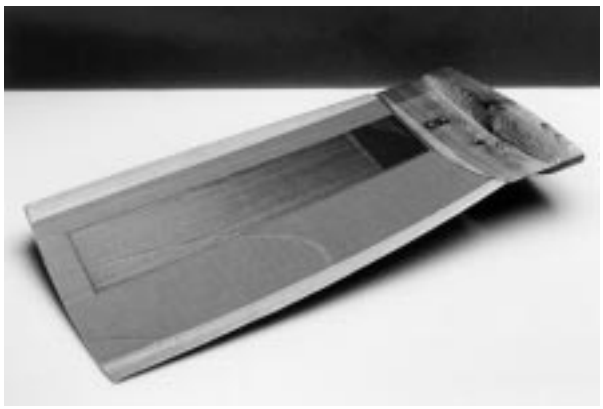

Fig. 6 Manufacture of HST composite blades. Rohacell core with lay-up of glue and carbon fibre sheets

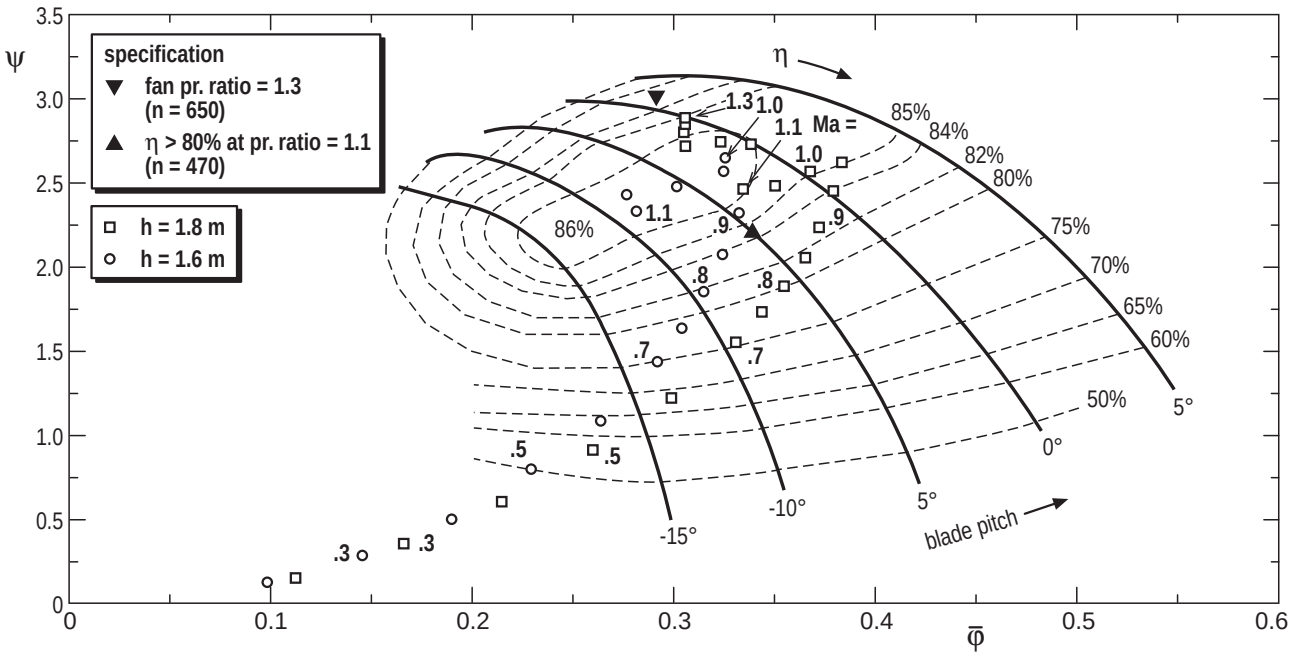

Fig. 5 Estimated fan characteristics from model rests

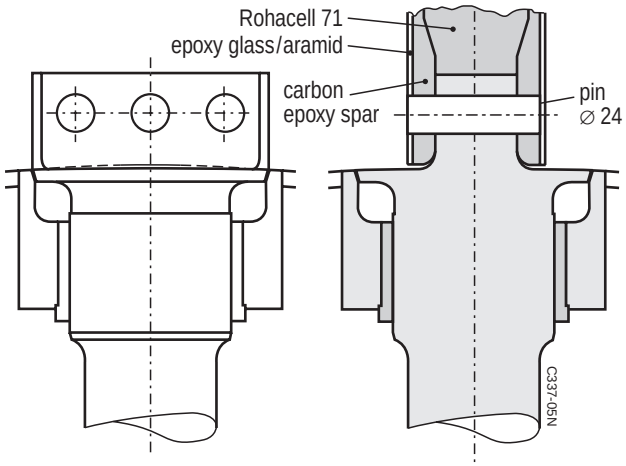

Fig. 7 Composite blade-steel spoke connection

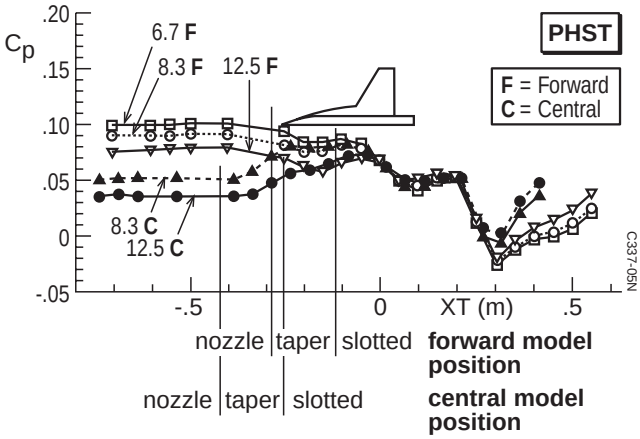

Fig. 9 Wall pressure measurements relative to model in PHST (Mach = .7: C_L = 1.3)

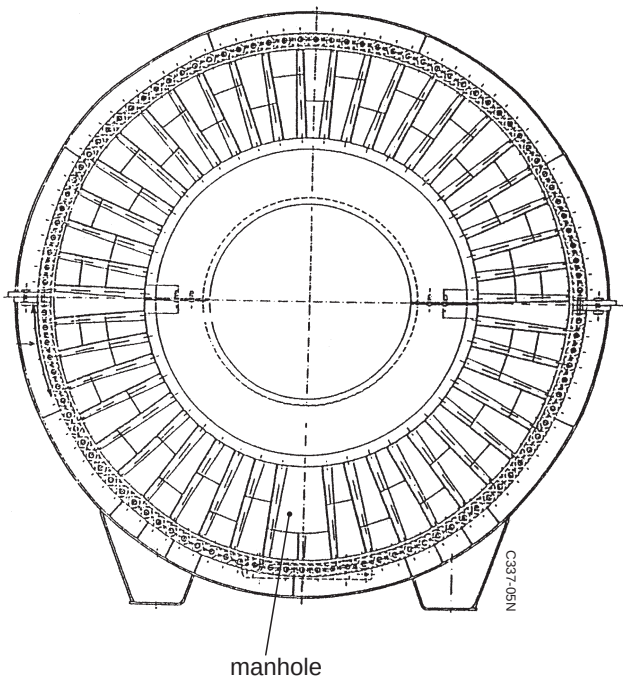

Fig. 8 Front view of stator vane arrangement

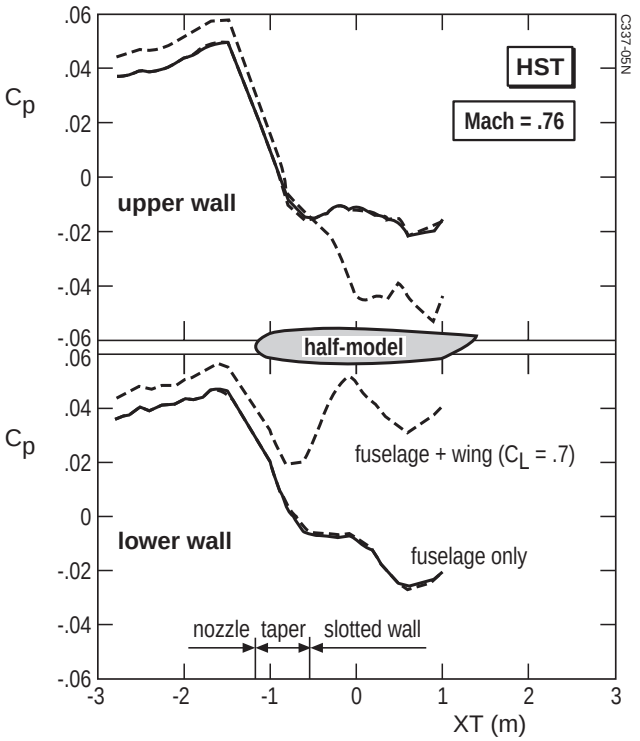

Fig. 10 Wall pressure measurements for half model in HST

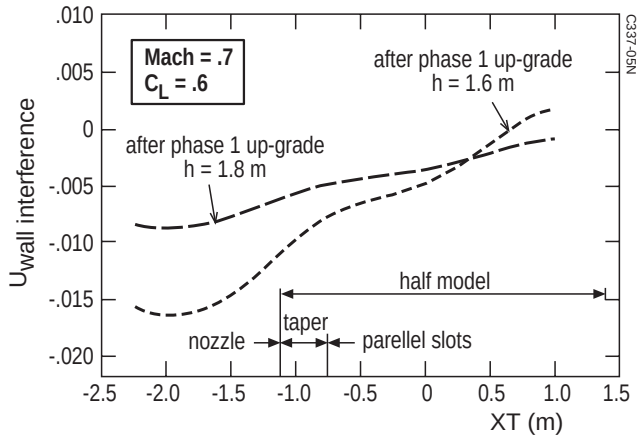

Fig. 11 Calculated wall interference velocity at halfmodel center line

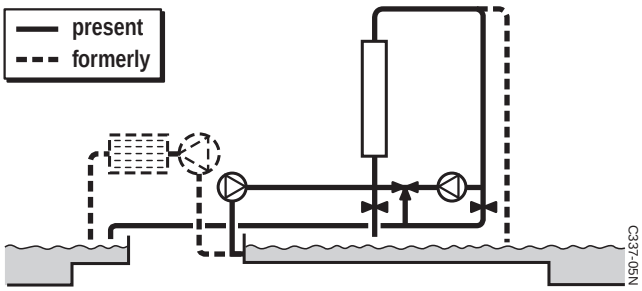

Fig. 13 Adaption to the cooling water system

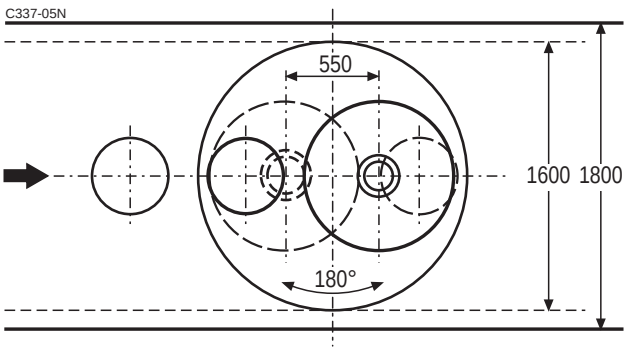

Fig. 12 Rearranging of the half model support

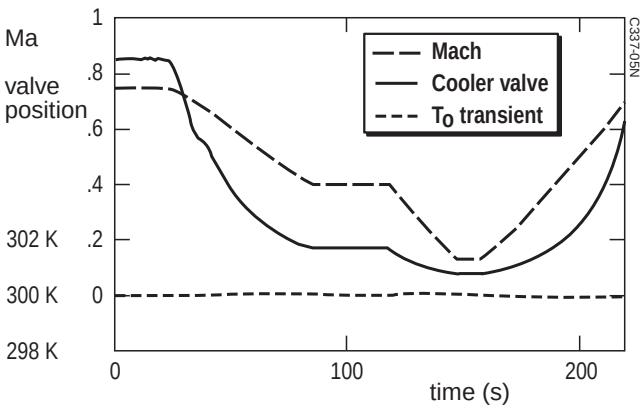

Fig. 14 Simulated total temperature control due to Mach number variation

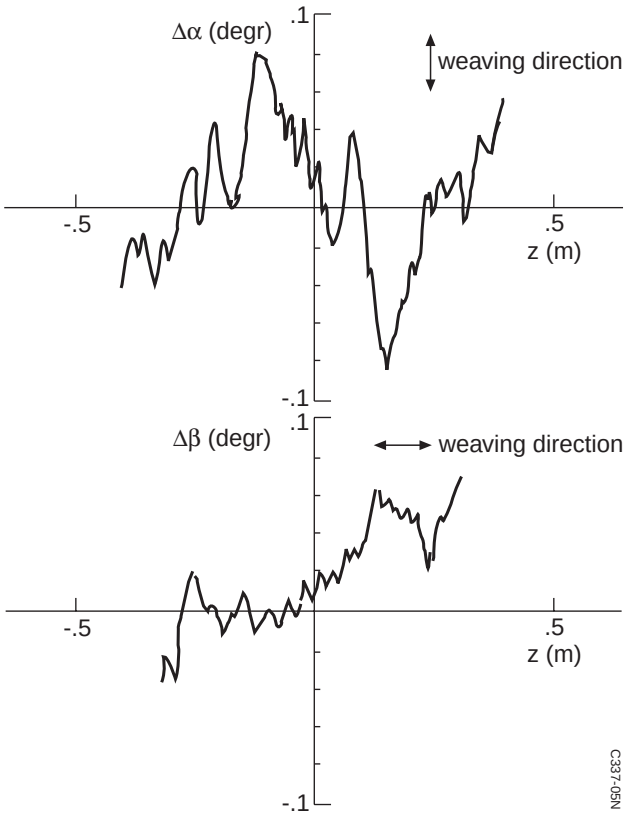

Fig. 15 Dependence of weaving direction of settling chamber screens on flow angularity (measured in LST)

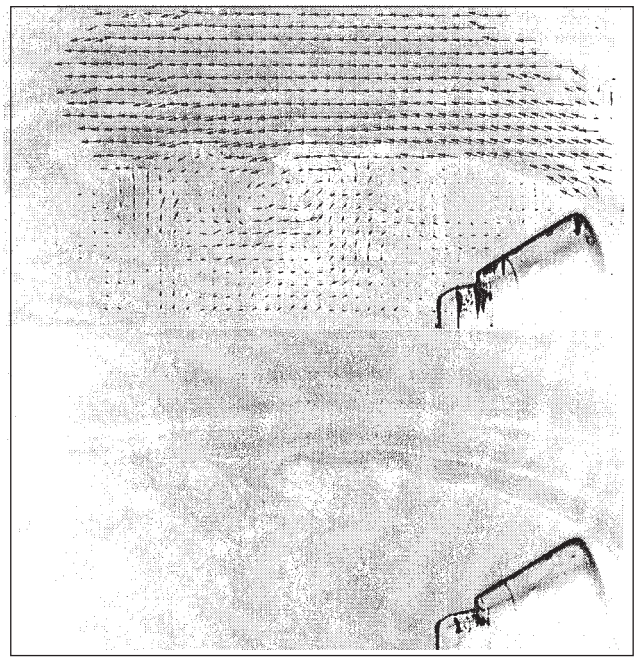

Fig. 17 PIV and flow picture of wake of re-entry capsule in HST, Ma = 0.5

Fig. 16 Two 40-bar aircompressors driven by 2 DOL motors

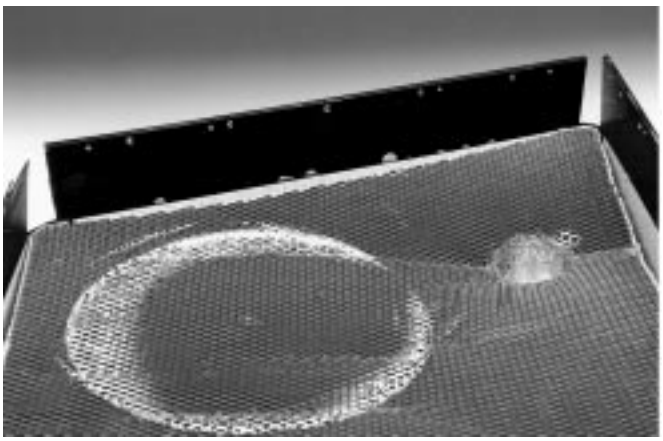

Fig. 18 Result of impact tests on panel of new foreign object detainer